Electronic Supplementary Material (ESI) for Polymer Chemistry.

Supporting Information

Synthesis of triphenylphosphine-based microporous organic nanotube frameworks supported Pd catalysts with excellent catalytic activity

*Yang Xu, Tianqi Wang, Zidong He, Aiqing Zhong, Wei Yu, Buyin Shi and Kun Huang**

School of Chemistry and Molecular Engineering, East China Normal University, 500 N, Dongchuan Road, Shanghai, 200241, P. R. China.

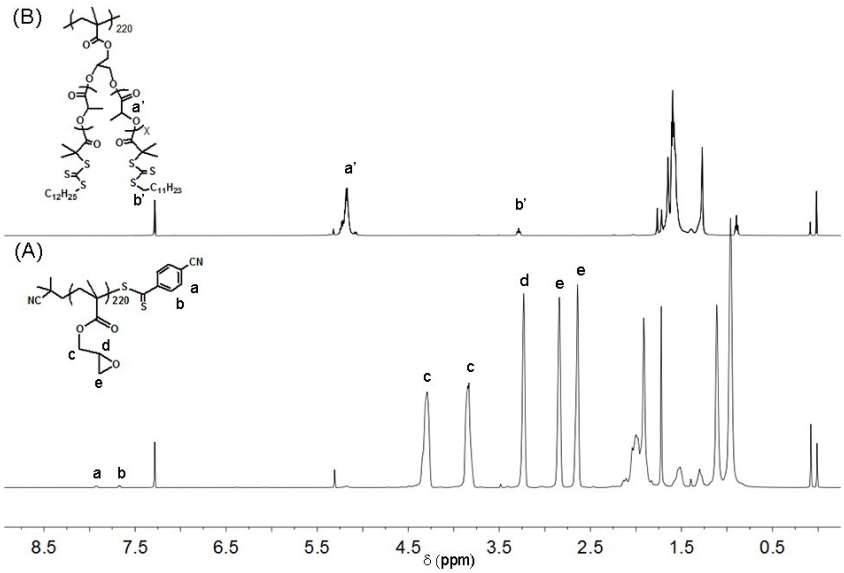

Figure S1. ^{1}H NMR spectra of (A) PGM and (B) poly(GM-g-LA).

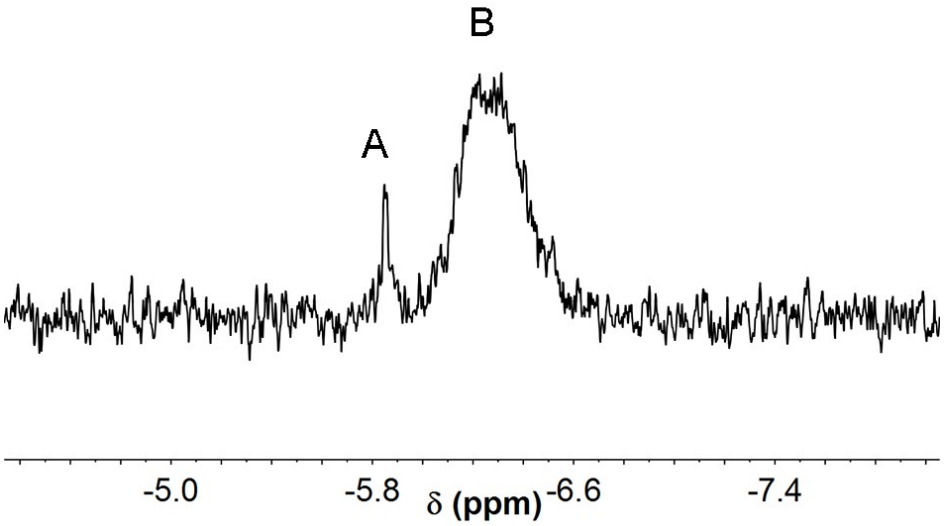

Figure S2. $^{31}P\{^{1}H\}$ NMR spectra of (A) DPPS monomer mixed with (B) copolymer precursors in $[D_8]THF$.

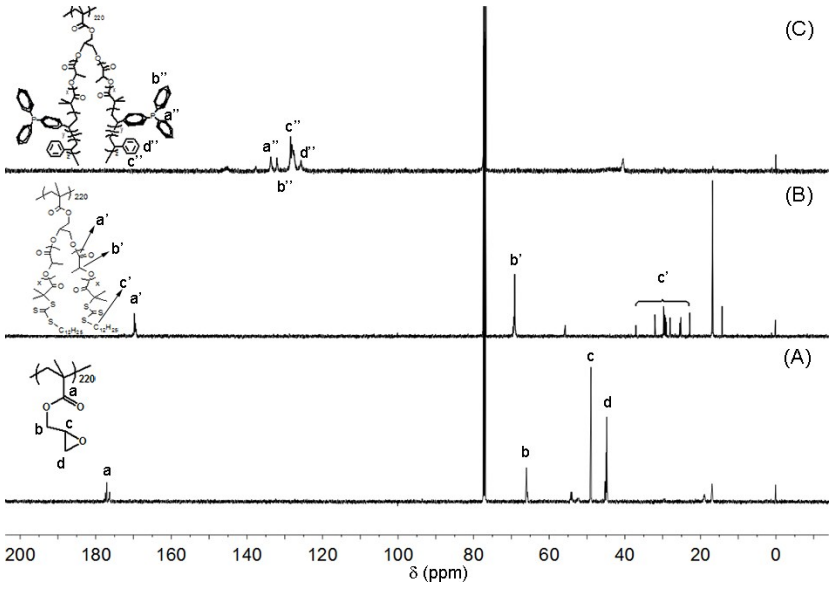

Figure S3. ^{13}C NMR spectra of (A) PGM, (B) poly(GM-g-LA) and (C) poly(GM-g-LA-g-S/DPPS).

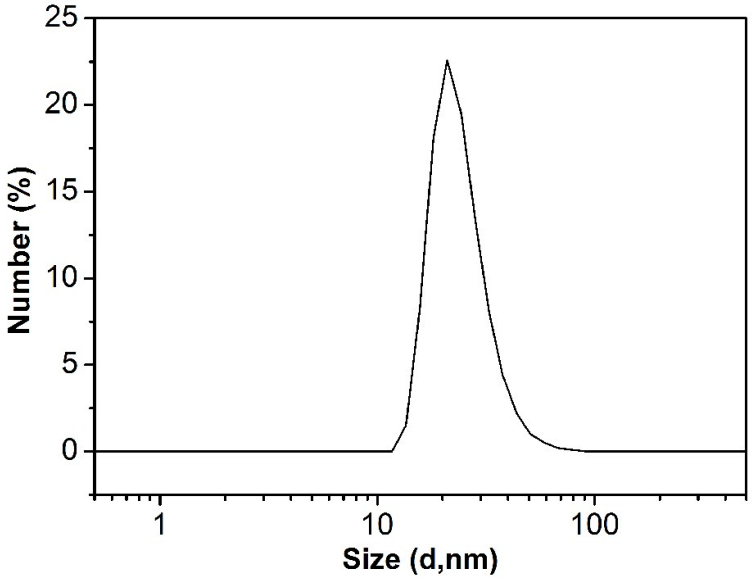

Figure S4. DLS analysis of poly(GM-g-LA-g-S/DPPS) bottlebrush polymer precursor in THF. Z-Average = 52 nm. PDI = 0.211.

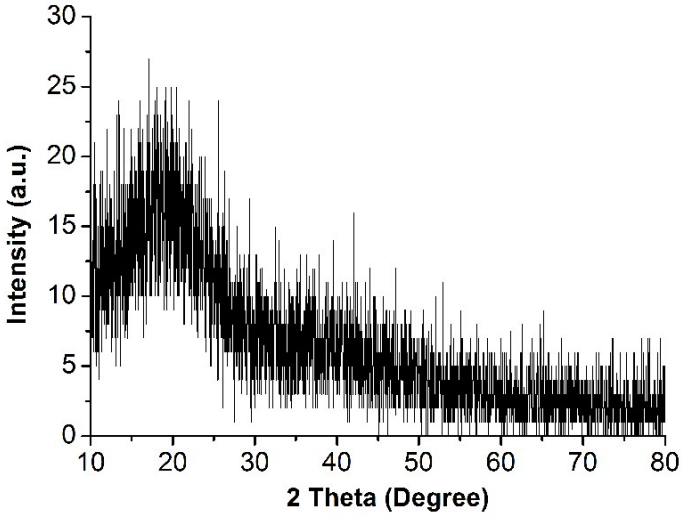

Figure S5. XRD pattern of MONFs-PPh_3@Pd.

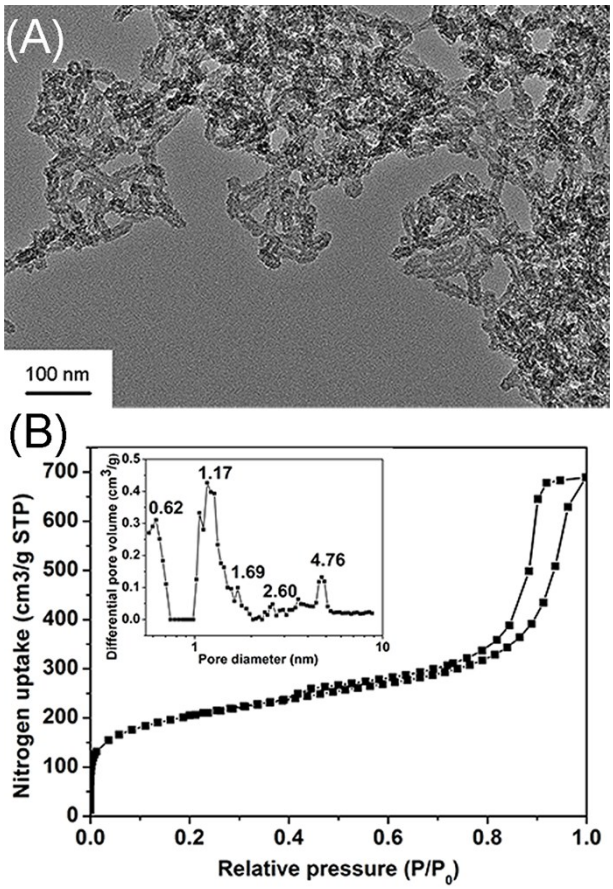

Figure S6. (A) TEM image and (B) N_2 sorption isotherm of MONFs-PPh_3@Pd-2. Pore size distribution was calculated by using the DFT methods provided inset.

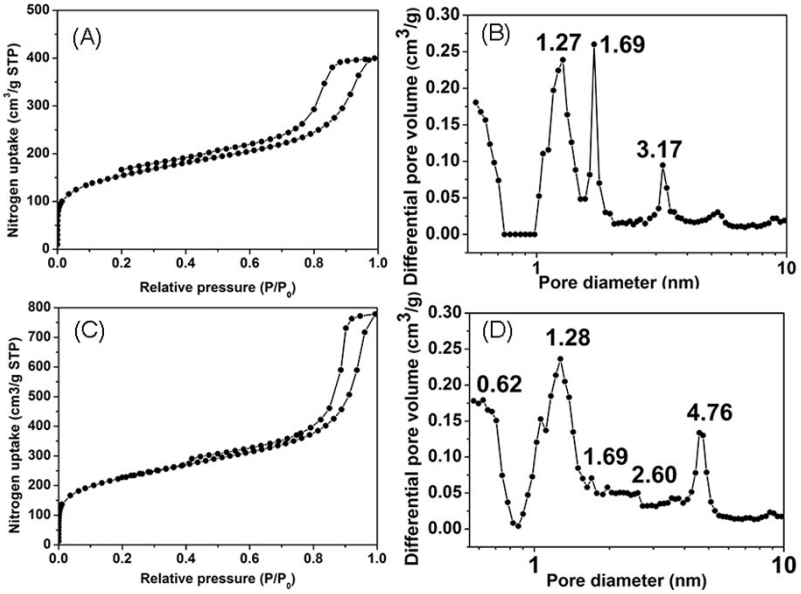

Figure S7. Nitrogen adsorption and desorption isotherms of (A) MONFs-PPh_3-1 and (C) MONFs-PPh_3-2. Pore size distributions calculated using DFT methods (slit pore

models, differential pore volumes. pore width) of (B) MONFs-PPh_3-1 and (D) MONFs-PPh_3-2.

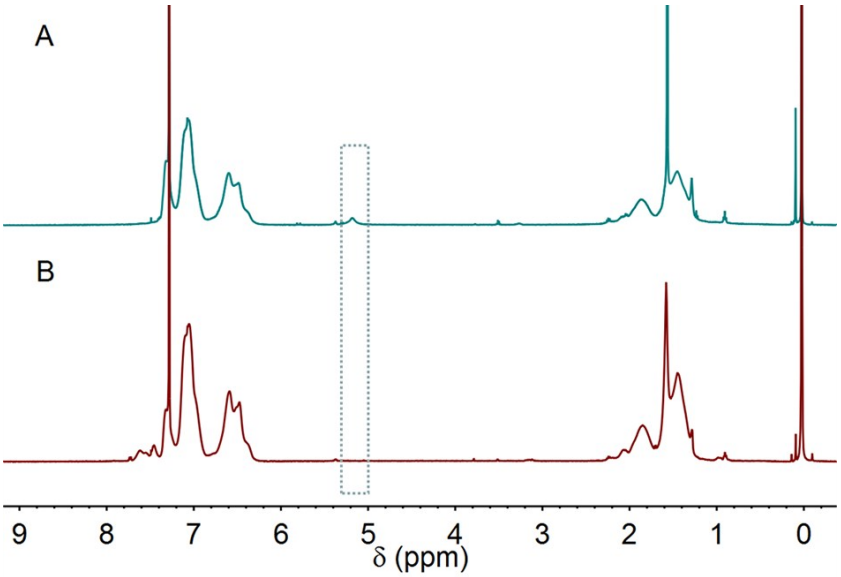

Figure S8. ^{1}H NMR characterization of (A) poly(GM-g-LA-g-S/DPPS) [precursor-1] and (B) S/DPPS block fragment from the precursor-1.

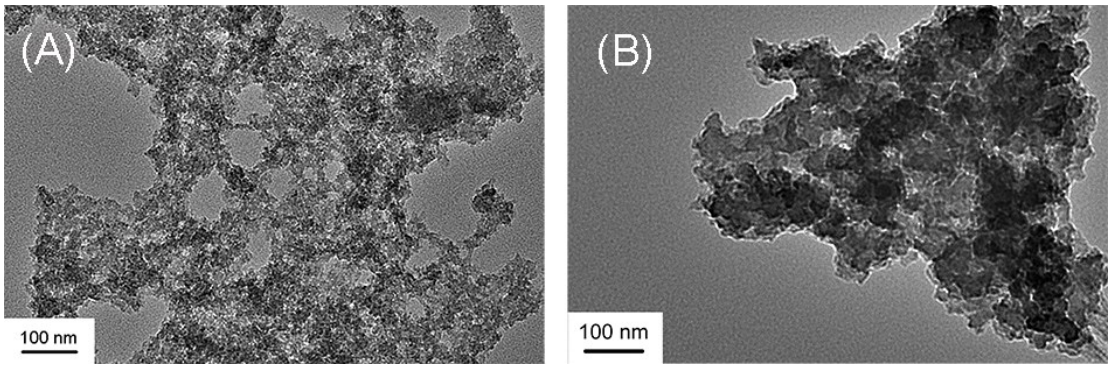

Figure S9. TEM images of (A) MOP-PPh_3@Pd and (B) MOP-PPh_3@Pd after 1st catalysis cycle.

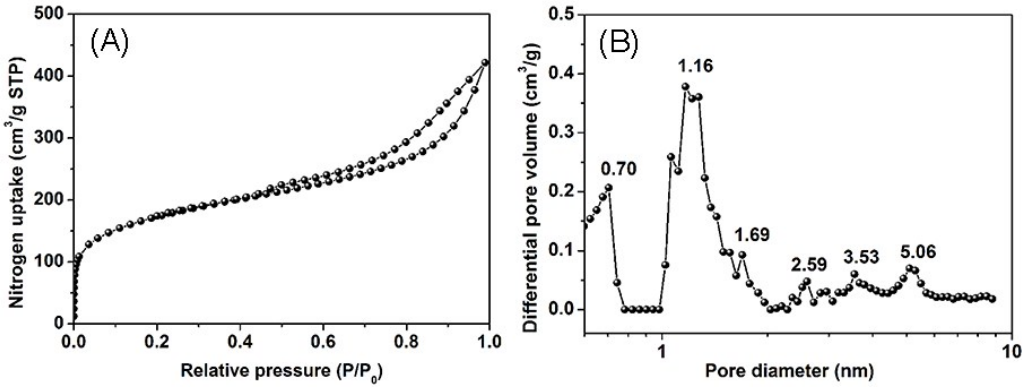

Figure S10. (A) Nitrogen adsorption and desorption isotherms; (B) Pore size distribution calculated using DFT methods (slit pore models, differential pore volumes. pore width) of MOP-PPh_3@Pd.

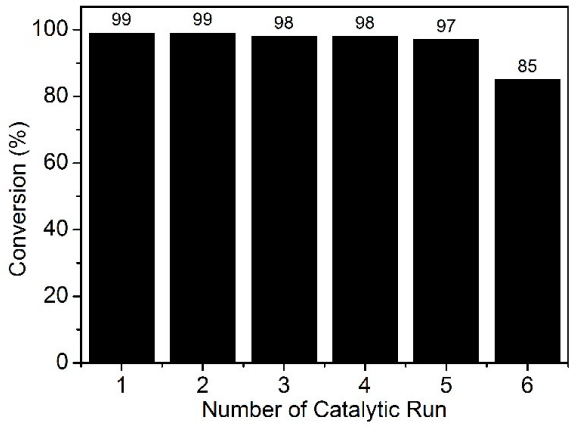

Figure S11. Recyclability and reusability of the MONFs-PPh_3@Pd-1 for the model reaction.

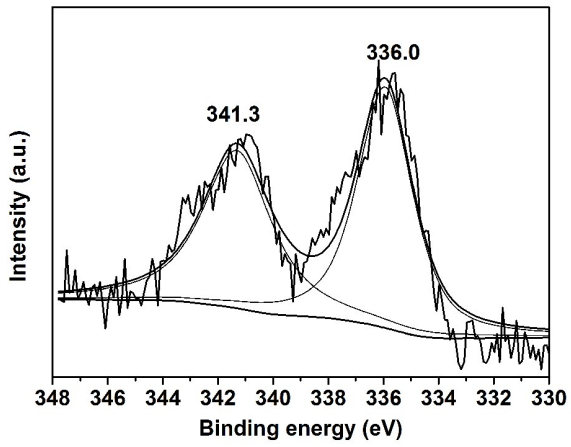

Figure S12. XPS spectra of Pd species in MONFs-PPh_3@Pd-1 after 5 runs.

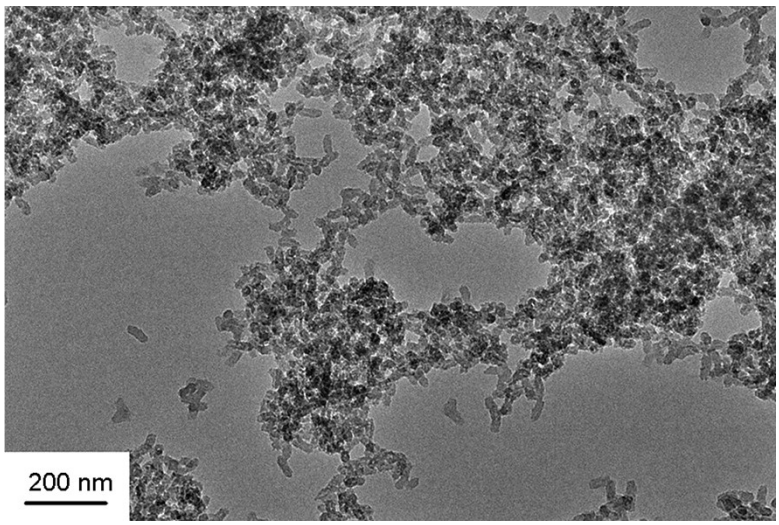

Figure S13. TEM image of MONFs-PPh_3@Pd-1 after 5 runs.

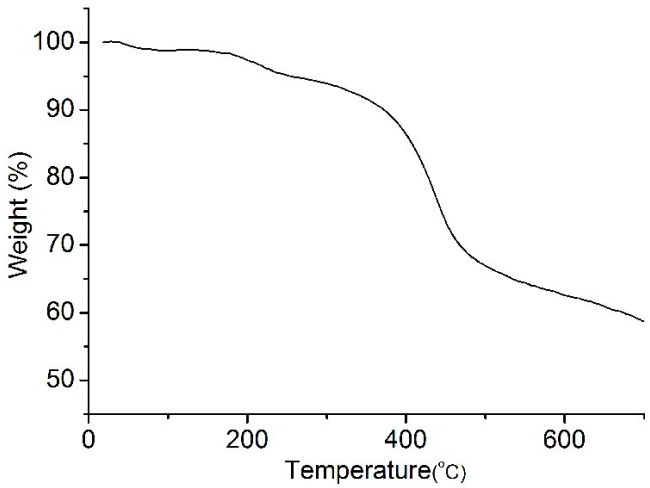

Figure S14. TGA analysis of MONFs-PPh_3@Pd-1.

Table S1. Porous properties comparison of different MONFs-based and MOP-based materials.

Samples	S_{BET} [m^2/g] [a]	S_{micro} [m^2/g] [b]	S_{meso} [m^2/g] [c]	V_{Total} [cm^3/g] [d]	Dp [nm] [e]
MONFs-PPh_3-1	542	179	363	0.73	1.27/3.17
MONFs-PPh_3@Pd-1	538	136	402	0.70	1.17/3.17
MONFs-PPh_3-2	763	225	538	1.21	1.28/4.76
MONFs-PPh_3@Pd-2	696	262	434	1.07	1.17/4.76
MOP-PPh_3@Pd	486	212	274	0.65	1.16/--

[a] BET specific surface area calculated from N_2 adsorption isotherm at 77.4 K; [b] Microporous surface area calculated from t-plots; [c] Mesoporous surface area; [d] Total pore volume at P/P_0 = 0.998; [e] Pore size calculated by density functional theory (DFT) methods (Microporous pore size/ Mesoporous pore size).

Table S2. Comparison of catalytic efficiency for catalytic Aryl chlorides model Suzuki-Miyaura coupling reaction with various Pd catalysts.

Catalyst	Pd mol%	Base	Reaction conditions	Yield/%	TOF/h^{-1}	Ref.
KAPs(Ph-PPh_3)-Pd	0.60	$K_3PO_4 \cdot 3H_2O$	EtOH/H_2O, 80°C, 3h, under N_2	99	55.0	1
Pd/MPP	0.20	K_2CO_3	EtOH/H_2O, 80°C, 24h, in air	<30 [a)]	--	2
Poly-NHC-2-Pd^{2+}	0.06	--	EtOH/H_2O, 80°C, 3h, in air	100	585	3
Pd/MIL-101	0.90	NaOMe	TBAB/H_2O, 80°C, 20h, under N_2	97	5.40	4
MOMP 4	0.50	K_2CO_3	H_2O, 80°C, 10h	92	18.4	5
Pd/POL-Ph_3P	2.00	K_2CO_3	Toluene, 80°C, 2h	96 [a)]	--	6
MONFs-PPh_3@Pd	0.12	K_2CO_3	EtOH/H_2O, 80°C, 3h, under N_2	99	275	This work

[a)] These isolated yields were calculated based on the cross-coupling reaction between p-chloroacetophenone and phenylboronic acid.

Analytical data for compounds of the Suzuki-Miyaura coupling reactions.

Biphenyl

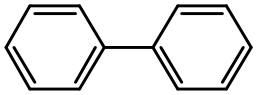

^{1}H NMR (500 MHz, $CDCl_3$): δ 7.59 (d, J = 7.5 Hz, 4H); 7.45 (t, J = 7.5 Hz, 4H); 7.35 (tt, 2H).

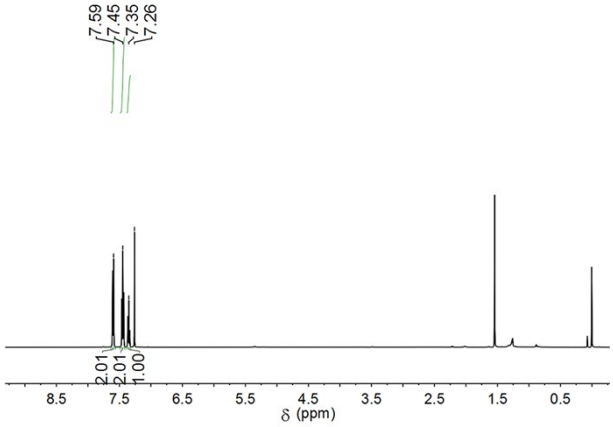

4-Acetylbiphenyl

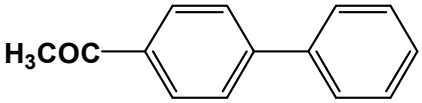

^{1}H NMR (500 MHz, $CDCl_3$): δ 8.04 (d, J = 8.5Hz, 2H); δ 7.69 (d, J = 8.5Hz, 2H); δ 7.64 (d, J = 8.5Hz, 2H); δ 7.44 (m, 3H); δ 2.64 (s, 3H).

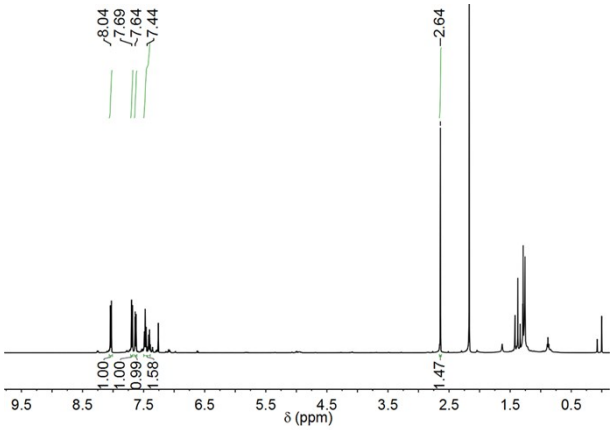

4-Nitrobiphenyl

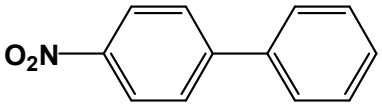

^{1}H NMR (500 MHz, $CDCl_3$): δ 8.30 (d, J = 8.5Hz, 2H); δ 7.74 (d, J = 8.5Hz, 2H); δ 7.62 (d, J = 7.5Hz, 2H); δ 7.50 (m, 3H).

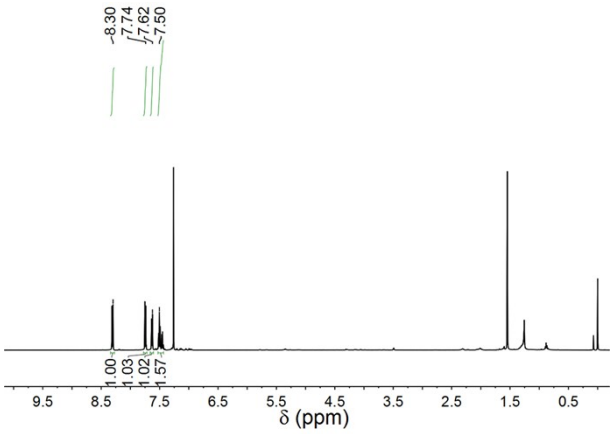

3-Nitro-1,1'-biphenyl

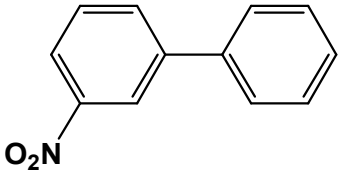

^{1}H NMR (500 MHz, $CDCl_3$): δ 8.46 (d, J = 2.0Hz, 1H); δ 8.20 (dq, 1H); δ 7.91 (dq, 1H); δ 7.62 (m, 3H); δ 7.49 (t, J = 8.0Hz, 2H); δ 7.44 (m, 1H).

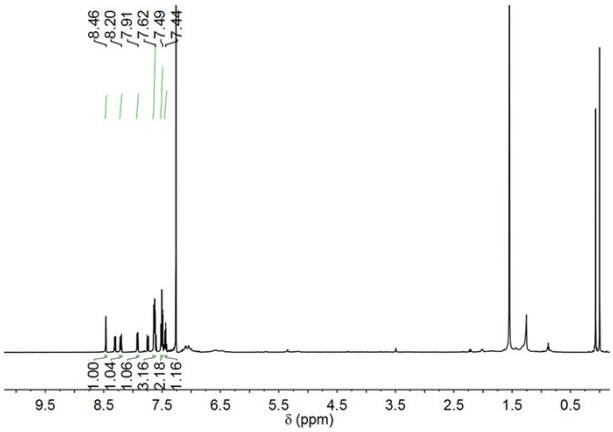

4-Methylbiphenyl

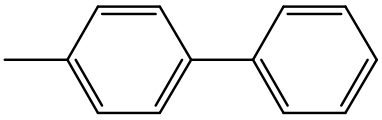

^{1}H NMR (500 MHz, $CDCl_3$): δ 7.58 (d, J = 8.0Hz, 2H); δ 7.49 (d, J = 8.0Hz, 2H); δ 7.43 (t, J = 7.5Hz, 2H); δ 7.31 (m, 1H); δ 7.25 (d, J = 8.0Hz, 2H); δ 2.39 (s, 3H).

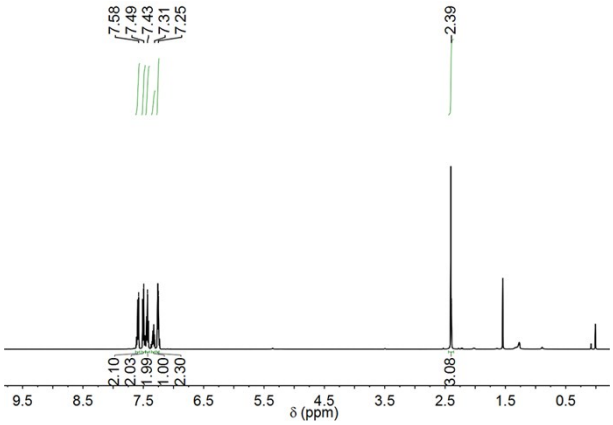

4-Methoxybiphenyl

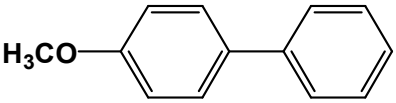

^{1}H NMR (500 MHz, $CDCl_3$): δ 7.55 (m, 4H); δ 7.42 (d, J = 7.5Hz, 2H); δ 7.31 (t, J = 7.5 Hz, 1H); δ 6.98 (d, J = 9.0 Hz, 2H); δ 3.86 (s, 3H).

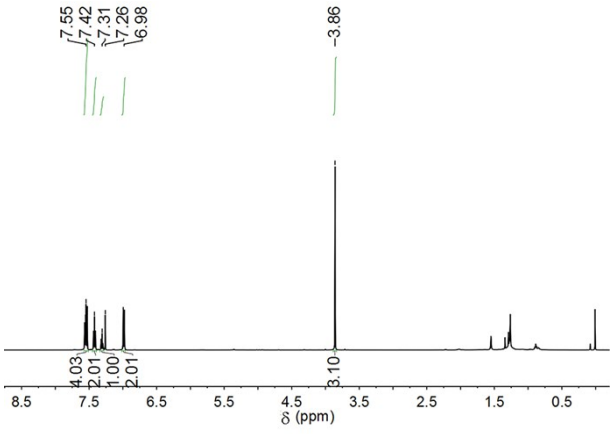

4-Trifluoromethylbiphenyl

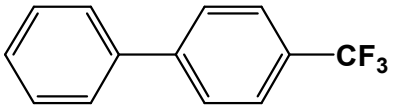

^{1}H NMR (500 MHz, $CDCl_3$): δ 7.70 (s, 4H); δ 7.59 (d, J = 8.0Hz, 2H); δ 7.42 (m, 3H).

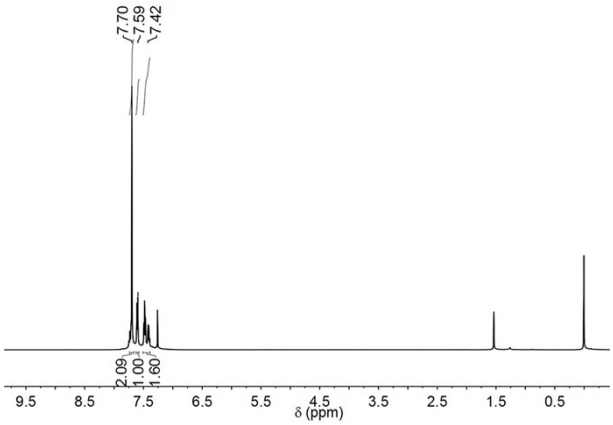

References

1. B. Li, Z. Guan, W. Wang, X. Yang, J. Hu, B. Tan and T. Li, *Adv Mater*, 2012, **24**, 3390-3395.
2. Q. Song, Y. Jia, B. Luo, H. He and L. Zhi, *Small*, 2013, **9**, 2460-2465.
3. S. Xu, K. Song, T. Li and B. Tan, *J. Mater. Chem. A*, 2015, **3**, 1272-1278.
4. B. Yuan, Y. Pan, Y. Li, B. Yin and H. Jiang, *Angewandte Chemie International Edition*, 2010, **49**, 4054-4058.
5. C. Zhang, J.-J. Wang, Y. Liu, H. Ma, X.-L. Yang and H.-B. Xu, *Chemistry - A European Journal*, 2013, **19**, 5004-5008.
6. Y.-B. Zhou, C.-Y. Li, M. Lin, Y.-J. Ding and Z.-P. Zhan, *Advanced Synthesis & Catalysis*, 2015, **357**, 2503-2508.